Asociación Argentina
de Mecánica Computacional

Mecánica Computacional Vol XXVI, pp.1440-1452
Sergio A. Elaskar, Elvio A. Pilotta, Germán A. Torres (Eds.)
Córdoba, Argentina, Octubre 2007

COHESIVE LAWS TO MODEL CONCRETE RUPTURE – A METHODOLOGY THAT TAKES MESH EFFECTS INTO CONSIDERATION

Luciani N. Lens[a], Eduardo Bittencourt[b], Virgínia M. R. d'Avila[b]

[a] *Centro de Ciências Exatas e Tecnológicas, Universidade Estadual do Oeste do Paraná, Campus de Cascavel, Rua Universitária 2069, Cascavel, PR, Brazil, lnlens@unioeste.br, http://www.unioeste.br*
[b] *Centro de Mecânica Aplicada e Computacional, Univesidade Federal do Rio Grande do Sul, Avenida Osvaldo Aranha, 99, Porto Alegre, RS, Brazil, bittenco@cpgec.ufrgs.br, http://www.ppgec.ufrgs.br/Cemacom*

Keywords: Fracture Mechanics, concrete, cohesive surfaces, finite elements.

Abstract. The cohesive surface method has been used intensively on numerical simulations of fracture of metals and brittle materials. However, the constitutive cohesive laws (or traction versus crack opening relationships) used for these materials are not adequate to simulate the concrete behavior because they do not take into consideration effects related to the size of the finite elements and other phenomena that characterize concrete rupture (e.g. development of a process zone at the crack tip).

In this work, some well-known post-peak constitutive equations for the cohesive surface are explored. The shape of these equations changes overall results and it seems to be linked with the development of the process zone, so the shape can be considered a material property as the fracture energy. However, the present work also explores the effect of the pre-peak part of the cohesive law. It is demonstrated that this part of the curve must be related to the size of the finite elements, in order to have a mesh independent result.

As practical applications, cases in Mode I of propagation are presented (three-point bending), where the effect of the post-peak relationship on load versus crack opening is shown. It could be concluded that post-peak relationship is important to define maximum rupture load. Besides that, different sizes of bodies were analyzed and the scale effect of concrete was captured (the smaller the body, the greater the toughness). A good fit with literature results was obtained. It is demonstrated also that results are mesh independent, depending on the pre-peak part of the cohesive law. Concrete properties are not considered random fields.

1 INTRODUCTION

Applications of the one-parameter Linear Elastic Fracture Mechanics (LEFM) to concrete are restricted due to the presence of the process zone. Then, two or more fracture parameters have been proposed to characterize concrete, such as in the "fictitious crack model" of Hilleborg et al. (1976), the "crack band model" of Bazant and Oh (1983) and the "two parameters" (K_{IC}, $CTOD_c$) method of Jenq and Shah (1985a), among many others.

The present work will focus on Hilleborg et al. ideas, implemented in a Finite Element (FE) context, where fictitious cracks are considered between each FE of the domain through cohesive zones or surfaces. The model for these zones is represented by a function of the tractions in terms of separation distances between FE faces, which corresponds to crack opening. According to de Borst et al. (2006), while for ductile fracture the most import factor of the cohesive surface model seem to be the tensile strength, for quasi-fragile material, where micro-cracking plays an important factor, the shape of the stress-opening relation of the crack appears to be more significant. Chandra et al. (2002) also claim that shape of stress-opening relation can not be neglected in the analysis of quasi-fragile materials. Finally, Tijssen et al. (2000) reported that fracture path of concrete is mainly determined by the initial slope of softening of the cohesive law. In fact, experimental results indicate that a concave curve with a steeper decline after the peak is the most adequate (Rots, 1988).

Then the fundamental material parameters in a cohesive model for concrete are the fracture energy and the shape of the traction versus crack opening. Although is polemic to say that fracture energy is a property in concrete structures due to size effects, Rots (1988) argued that, in general, objections against the use of the fracture energy as a concrete property are exaggerated, since has been reported that increases in size up to eight times do not change fracture energy more than 20 percent.

One aspect of the application of cohesive surfaces to concrete that is rarely mentioned is the pre-peak or elastic part of the constitutive law. As all such methodologies follows the basic principles of Barrenblat (1962) and Dugdale (1960), this elastic part must exist. In Rots (1988) it is mentioned only that this part is arbitrarily small. In applications to fragile and ductile materials, the elastic part is considered a material property (see Needleman, 1987 and Xu and Needleman, 1990). It was already demonstrated that these constitutive laws are not suited to concrete (see Lens et al. 2006). As we will see later, the elastic part must be mesh dependent in quasi-fragile materials to eliminate mesh dependency.

The constitutive laws used in this work for the cohesive surfaces are presented and described in chapter 2; implementation in a FE framework is described in chapter 3; chapter 4 shows applications of the methodology for three-point bending cases, mode I propagation. Concluding remarks are done in chapter 5.

2 CONSTITUTIVE LAWS FOR COHESIVE SURFACE

As mentioned above, to represent crack behavior is necessary to establish a relationship between tractions and opening of the surfaces. It is known that when surfaces start to separate from each other, tractions increase reaching a peak value. Afterwards tractions decrease until reach a zero value for crescent opening. For this opening the surfaces are considered fractured. This behavior occurs in different scales, from separation of atomic planes, as described for instance by Rose et al. (1981), to macro-scale at the crack tips, as described by Barrenblat (1962), Dugdale (1960). Depending on the scale or material being represented by separation of the surfaces, different peak tractions, peak and final openings are used. A vast collection of such values can be found in Chandra et al. (2002). In the case of concrete, the

subject of this work, we separate the constitutive law of cohesive surfaces in two parts: the post-peak and the pre-peak part as follows.

2.1 Post-peak of the constitutive law

Three shapes of post-peak constitutive laws are represented below: Hillerborg et al. (1976), CEB-FIP Code Model (1993) and Xu (1999). These relationships are implemented in the present work in the cohesive surface context and are depicted in Figure 1.

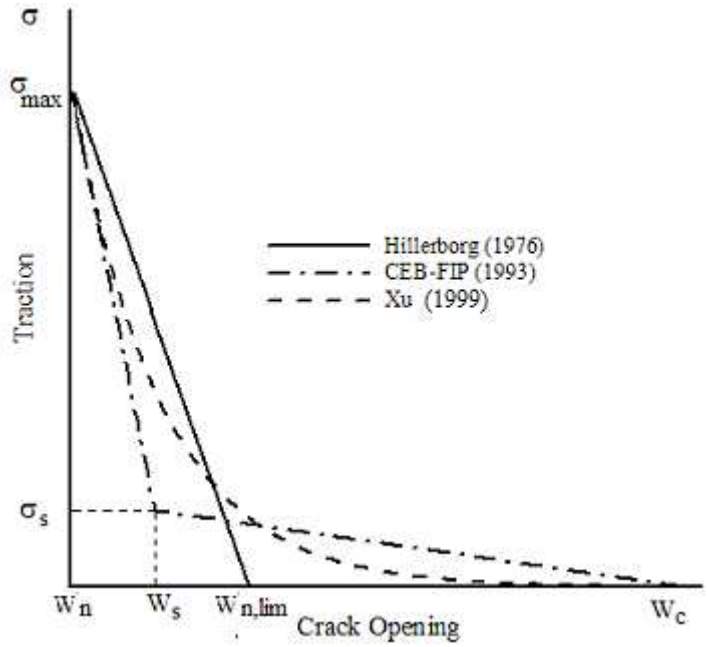

Figure 1: Post-peak cohesive surface constitutive law.

The shape of post-peak traction-opening seems to be linked with the development of the so called process zone where many complex phenomena occur such as micro-cracking, interlock bridging, friction between surfaces and agregates, etc. The area under the curve is considered the fracture energy (ϕ_n) and the maximum traction (σ_{max}) is related to the tensile strength. Interesting that the shape of post peak has an important influence on results (such as the maximum load achieved), as will be seen in chapter 4. There are some practical indications that this curve should be steeper for smaller openings, due to intense micro-cracking, and much less steep for large openings due to bridging or interlock effects (Rots, 1988 and Tijssen et al. 2000). Then, theoretically, among the three cases studied, the curve of Hilleborg et al. would be the less suited for concrete. This issue will be addressed again in chapter 4.2.

The equation for normal traction (σ_n) for Hilleborg et al. post-peak is:

$$\sigma_n = \frac{\sigma_{max}}{\left(w_{n,lim} - w_n\right)}\left(w_{n,lim} - w\right) \Rightarrow \left(w_n < w \le w_{n,lim}\right), \quad (1)$$

where w is the normal opening, w_n the elastic opening and $w_{n,lim}$ the final opening (where the interface cracks), that can be calculated as follows:

$$w_{n,lim} = \left(\frac{2\phi_n}{\sigma_{max}} + w_n \right). \quad (2)$$

The equations of the bi-linear model of CEB-FIP (1993) is described below:

$$\sigma_n = \frac{0,85\sigma_{max}}{(w_s - w_n)}(w_s - w) + (0,15\sigma_{max}) \Rightarrow \ (w_n < w \leq w_s), \quad (3)$$

$$\sigma_n = \frac{0,15\sigma_{max}}{(w_c - w_s)}(w_c - w) \ \Rightarrow \ (w_s < w \leq w_c), \quad (4)$$

w_s and σ_s are the intermediate values shown in Figure 1, while the final opening is named w_c. These values are calculated as follows:

$$w_c = \frac{7\phi_n}{\sigma_{max}}, \quad (5)$$

$$\sigma_s = 0,15\sigma_{max}, \quad (6)$$

$$w_s = \frac{2\phi_n}{\sigma_{max}} - 0,15w_c + w_n. \quad (7)$$

Finally, the exponential Xu (1999) expression is given below:

$$\sigma_n = \sigma_{max} \exp\left(-\eta \left(\frac{w - w_n}{w_c} \right) \right) \ \Rightarrow \ (w_n < w \leq w_c), \quad (8)$$

where,

$$\eta = \alpha_F \left[1 - \exp(-\alpha_F) \right], \quad (9)$$

$$\alpha_F = \lambda - \frac{(d_{max})^{0,9}}{8}, \quad (11)$$

$$\lambda = 10 - \left(\frac{f_{ck}}{20} \right)^{0,7}, \quad (10)$$

and

$$w_c = \alpha_F \frac{\phi_n}{\sigma_{max}}, \quad (12)$$

d_{max} (mm) is the maximum aggregate diameter and f_{ck} (MPa) the characteristic compressive strength.

The fracture energy is represented here by the normal work of separation of the cohesive surface, ϕ_n, since Mode II and III of propagation are not considered. ϕ_n depends on several factors, but the most representative (Xu,1999) are f_{cm} and d_{max}. (f_{cm} is the average compression strength and is taken as f_{ck}+8 MPa). Then, when experimental information about fracture energy is not available, ϕ_n can be determined by Equation (13) (see Xu,1999) as follows (d_{max} in mm and f_{cm} in MPa).

$$\phi_n = 0,0204 + 0,0056 \frac{d_{max}^{0,95}}{8} \left(\frac{f_{cm}}{10} \right)^{0,7}. \tag{13}$$

Based on previous studies (Lens et al., 2006), σ_{max} should range from 1 to 3 times the average tensile strength of the concrete, f_{tm}. Actually this range was also used by Carpinteri et al. (2003). According to these authors the relation σ_{max} x f_{tm} depend on the size of the body (σ_{max} =f_{tm} for large specimens and σ_{max} =3 x f_{tm} for small specimens).

2.2 Pre-peak of the constitutive law

In the curves showed in Figure 1, the pre-peak portion is not depicted (crack opening from zero to w_n) This part of the curve is a non-dissipative elastic part of the surface opening. According to Rots (1988), w_n should be a small value in order that the elastic deformation of the cohesive surface be negligible compared to continuum elastic deformation. More important, we believe w_n should be a size dependent dimension, in order to avoid the introduction of an undesirable size effect, as depicted in Figure 2.

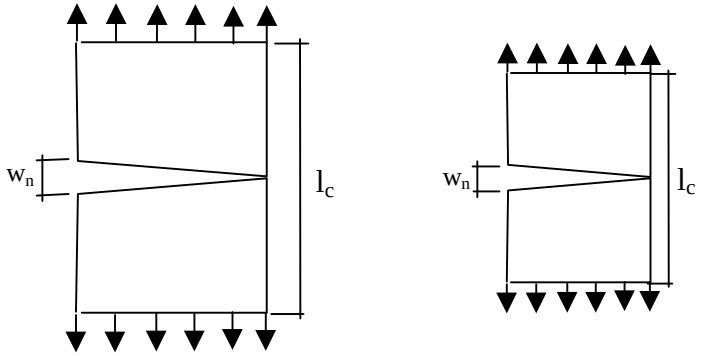

Fig. 2: Scaling of elastic opening w_n with size.

We propose here that,

$$w_n = \alpha \frac{\sigma_{max}}{E} l_c \tag{14}$$

or

$$w_n = \alpha \varepsilon_{max} l_c, \tag{15}$$

where $\varepsilon_{max} = \sigma_{max}/E$ is the elastic deformation of the continuum at the peak load (in Mode I) and l_c is its characteristic length. α should be a small value (in general $\alpha << 1$). In a FE context, l_c is taken as the characteristic length of the FE at the fracture zone. The use of a constant w_n value would introduce an undesirable mesh dependence on results when cohesive surfaces are used between all FE. In a successive remeshing process, still for w_n constant, no matter this value is small, at certain point the sum of all w_n will be greater than the elastic

volumetric displacements, which does not make sense. Another effect, maybe even more drastic, is the induction of a fake pure brittle behavior. Imagine a case as depicted in Figure 3. According to Carpinteri (1989), a transition from normal softening or quasi-fragile behavior to catastrophic softening occurs when $\varepsilon_{max}\, l_c$ is greater than w_c. As in the cohesive surface method an elastic part is introduced, this condition should be replaced by $\varepsilon_{max}\, l_c + w_n$ greater than w_c. This effect is shown in Figure 3, below.

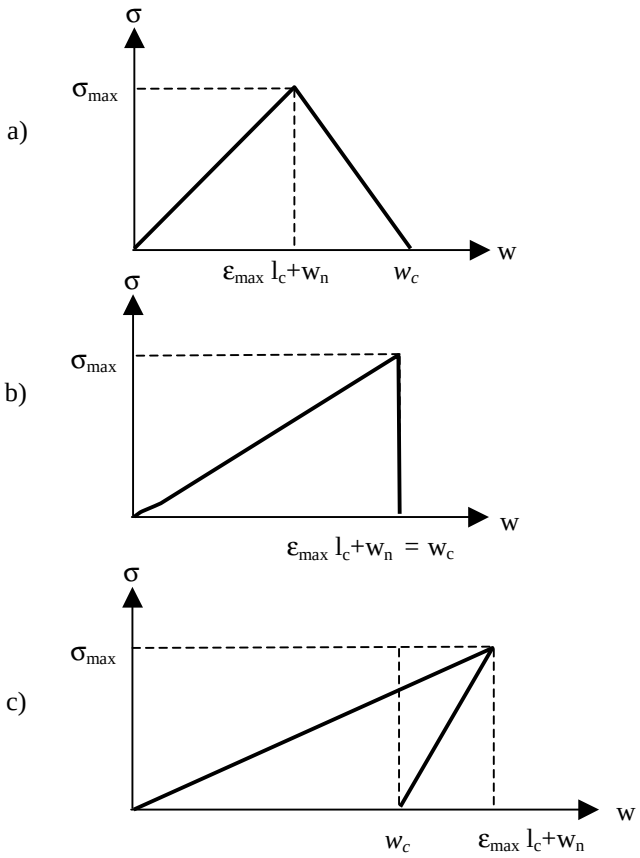

Fig. 3: Overall σ x w behavior of a bar in Mode I. Transition from quasi-brittle behavior (case a) to brittle or catastrophic behavior (cases b and c), induced by increased elastic displacement.

When transition described above is due to increase of l_c, it is the well known size effect in concrete. However, if this effect is caused by w_n, it represents only a numerical effect. This effect should not be confused with the spurious mesh sensitivity that occurs in smeared crack approaches, as described in Carpinteri et. al. (2003).

3 FINITE ELEMENT IMPLEMENTATION

The fracture behavior is here analyzed using the FEM together with cohesive elements (Xu and Needleman,1994) throughout the whole continuum. Considering an interface opening $\{\Delta\}$ in bi-dimensional problems, $\{T\}$ tractions, $\{n\}$ the normal vector and $\{t\}$ the tangent vector to the interface, it can be defined that:

$$\begin{aligned} w &= \{\Delta\}.\{n\}, \\ \sigma &= \{T\}.\{n\} \end{aligned} \tag{16}$$

and

$$z = \{\Delta\}.\{t\},$$
$$\tau = \{T\}.\{t\}, \tag{17}$$

(parenthesis {.} are used to represent vectors and brackets [.] to represent second order tensors). The cohesive normal traction σ arises as a result of the opening according to equations (1), (3-4) and (8), depending on the post-peak relation used (a linear equation is used for the pre-peak part). A linear equation is used for tangential tractions τ. σ and τ can be considered corotational tractions and then objective related to rigid body rotations, since they are integrated in the local system (n,t).

In this work the concrete is considered an elastic Hookean material. Damage can occur only by separation of interfaces in tension. No compressive damage is considered. The objective Jaumann stress rate $\left[\overset{\nabla}{\sigma}\right]$ is related to constitutive equation as follows:

$$\left[\overset{\nabla}{\sigma}\right] = [\Psi]\left[D^e\right], \tag{18}$$

where $[\Psi]$ is the Hooke tensor and $[D^e]$ the rate of deformation. The use of Jaumann stress rate in equation (18), together with corotational cohesive tractions (equations 16 and 17) enable the use of the formulation in large displacements. The Principle of Virtual Work including cohesive tractions, can be written as (body forces are neglected):

$$\int_\Omega [\sigma] : \left[\frac{\partial \delta U}{\partial X}\right] dV - \int_{\Gamma_f} \{F\}.\{\delta U\}\, dS + \int_{\Gamma_f} \{T\}.\{\delta \Delta\}\, dS = 0. \tag{19}$$

Constant triangular FE elements are used. The equation above is integrated in each FE volume Ω using one Gauss point, where {U} are nodal displacements, {F} are prescribed forces on boundary Γ_f. Tractions {T} are calculated in all FE faces using four Gauss points; integration is performed over the crack surface Γ_t. An implicit Newton-Raphson scheme is used to solve the corresponding equilibrium equations.

4 NUMERICAL EXPERIMENTATION

Examples of application of the theory are divided in two parts. First it is shown how mesh change results. Afterwards, size effects in concrete pieces are investigated and results are compared with literature.

4.1 Mesh dependency

In this section a three-point bending test is used to test mesh sensitivity. The size and boundary conditions are defined in the Figure 4 below, where S=190 mm; a=12 mm; D= 76 mm, L'= 12 mm, Ho=1 mm, ΔU=0.002 mm and B=38 mm. Concrete properties are E=23340 MPa, f_{ck}=25.2 MPa and ν=0.20. Cohesive surface properties are ϕ_n=100 N/m, σ_{max}=1.8 MPa and α=0.333. Three meshes are used here according to Figure 5.

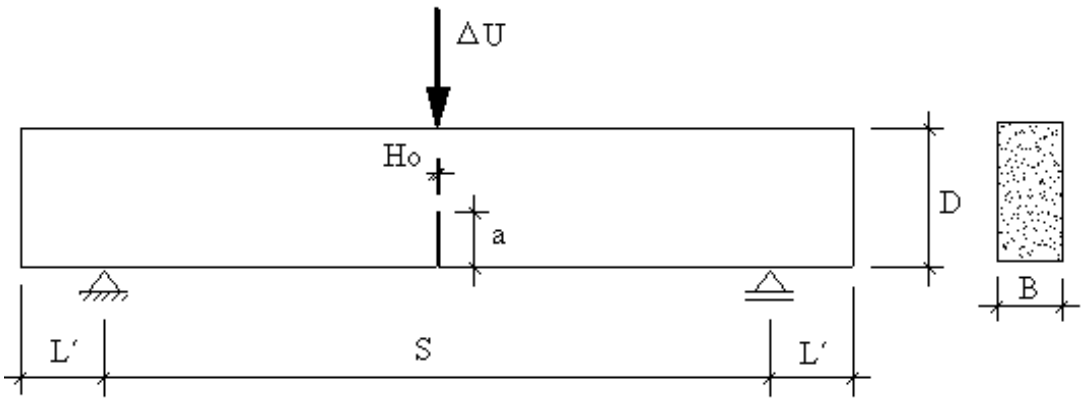

Figure 4: Geometry and boundary conditions.

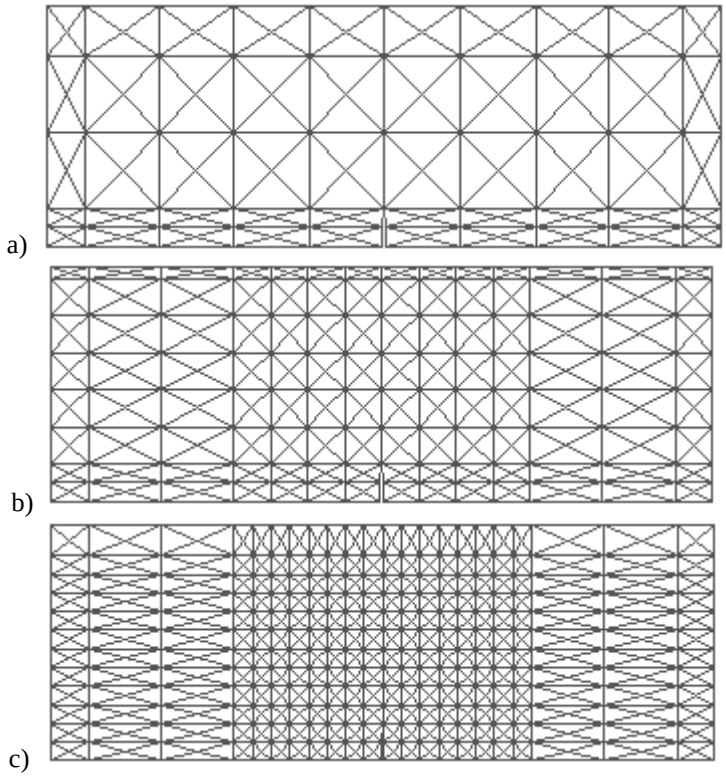

Figure 5: a) Coarse mesh ; b) medium mesh ; c) fine mesh.

Figure 6 shows results of load x crack opening and load x displacement, considering w_n constant, where l_c=12 mm and α=0,333. It can be observed a severe dependency of results on mesh size, being the fine mesh much more flexible than the coarse mesh, as expected. Also can be noticed that the fine mesh has the tendency to behave more brittle than coarse mesh, due to the effect mentioned in chapter 2.2 and shown in Figure 3 (peak load moves toward a large opening/displacement). This effect tends to disappear for smaller values of α. However, if mesh is also refined, the problem persists.

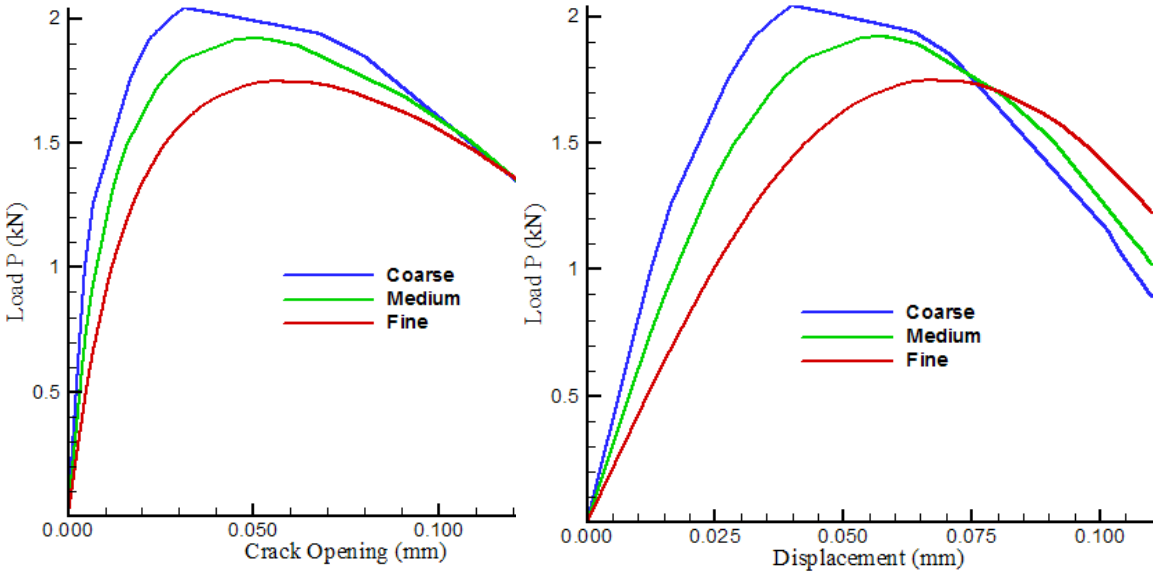

Figure 6: a) load x crack opening and b) load x displacement, considering w_n constant and different mesh resolutions.

In Figure 7, l_c is taken the characteristic length of each mesh. We observe that mesh effects practically disappear. In the case of the Figure 7, α=0.333, again. Another interesting outcome of the Figure 7, is that it somehow shows that post-peak interface properties do not need to be a function of the FE size. It is claimed by some authors (e.g. Iturrioz and Riera, 2005) that post-peak constitutive equation for concrete should be dependent on FE size. At least in the present way of considering concrete fracture, it does not seem necessary to consider such dependency.

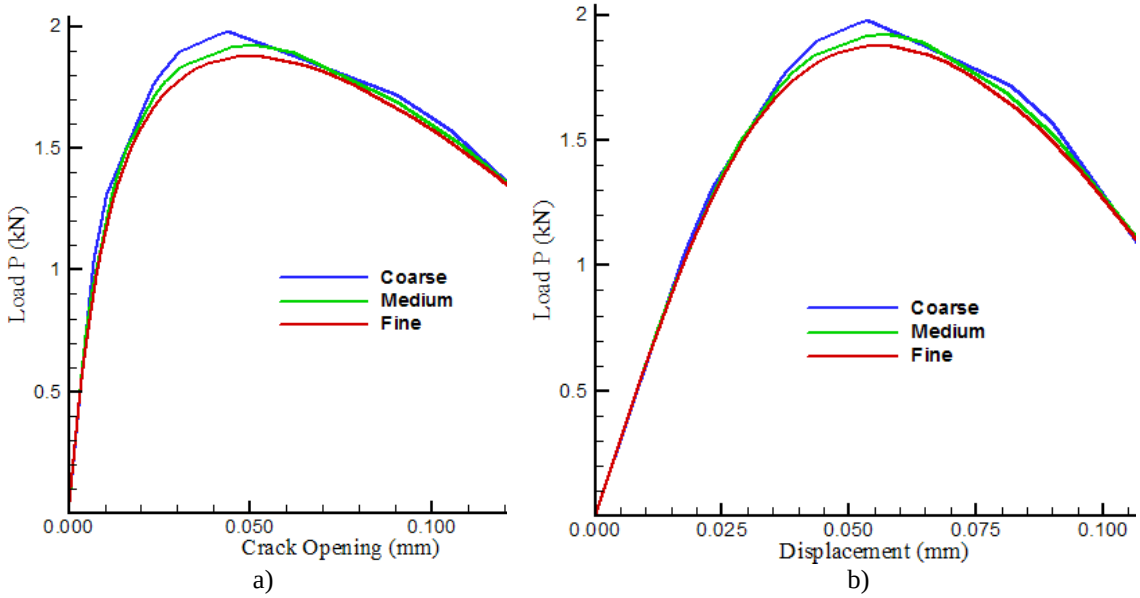

Figure 7: a) load x crack opening and b) load x displacement, considering w_n according equation (15) and different mesh resolutions.

4.2 Size effects

Two cases are considered here and compared with the literature. Both are three-point bending test, see Figure 4.

In the first case the geometric parameters are presented in Table 1. Concrete properties are E=27600 MPa, f_{tm}=2.9 MPa and ν=0.20. Cohesive surface properties are ϕ_n=66,27 N/m, σ_{max}=8.7 MPa, l_c=6 mm and α=1.

Specimens	S (mm)	D (mm)	B (mm)	L´(mm)	a (mm)	a/D	Ho (mm)
SH1	95	38	38	6	6	0.1667	3
SH2	190	76	38	12	12	0.1667	3
SH3	380	152	38	25	25	0.1667	3
SH4	760	304	38	50	50	0.1667	3

Table 1:Geometry of the first case.

Table 2 shows a comparison between experimental results (Shah et al., 1995) and the present theory.

Specimens	D	Maximum load (kN) results, Shah et al. (1995)				Maximum load (kN)	Difference %
	(mm)	Beam 1	Beam 2	Beam 3	Mean	Present study	
SH1	38	1.80	1.81	1.85	1.820	1.81	-0.55
SH2	76	3.01	3.14	3.16	3.103	3.65	+17.63
SH3	152	4.40	4.63	4.88	4.637	4.97	+7.18
SH4	305	7.73	7.74	7.89	7.787	7.80	+0.17

Table 2:Experimental results (Shah,1995) and the present theory for the first case.

A general good fitting was obtained. However a more complete comparison was necessary in order to verify the present theory, so a second case was studied and results compared with Jenq and Shah (1985b). In this case geometry parameters are presented in Table 3. Concrete and cohesive surface properties are in the Table 4. Observe that experimental elastic modulus (E) changes with size (Jenq and Shah 1985b).

Specimens	S (mm)	D (mm)	B (mm)	L´(mm)	a (mm)	a/D	Ho (mm)
JS1	305	76	29	12	25	0.333	1
JS2	610	152	57	25	50	0.333	1
JS3	914	229	86	38	76	0.333	1

Table 3:Geometry of the second case.

Specimens	f_{ck} (MPa)	E_c (MPa)	ϕ_n (N/m)	l_c (mm)	$\sigma_{máx}$ (MPa)	α
JS1	25.2	21.93	100	6	3.4259	0.125
JS2	25.2	23.34	100	6	3.4259	0.125
JS3	25.2	34.92	100	6	3.4259	0.125

Table 4: Concrete and cohesive surface properties of the second case.

Figure 8 shows the complete curve load x crack opening together with experimental curves (sub-index indicates the cohesive law used in the numerical model: H for Hillerborg et al., E for Xu (1999) and C for the CEB-FIP, 1993).Some interesting conclusions can be addressed inspecting the figure. First, the size effect is, indeed, captured. It can be noticed that curves load x crack opening are not similar, indicating the change in failure behavior as size changes. For the greatest body, load decrease much faster than in the smallest body, indicating the

trend of a sudden or brittle behavior when the body size is increased. Actually, the smallest body presents practically a ductile fracture.

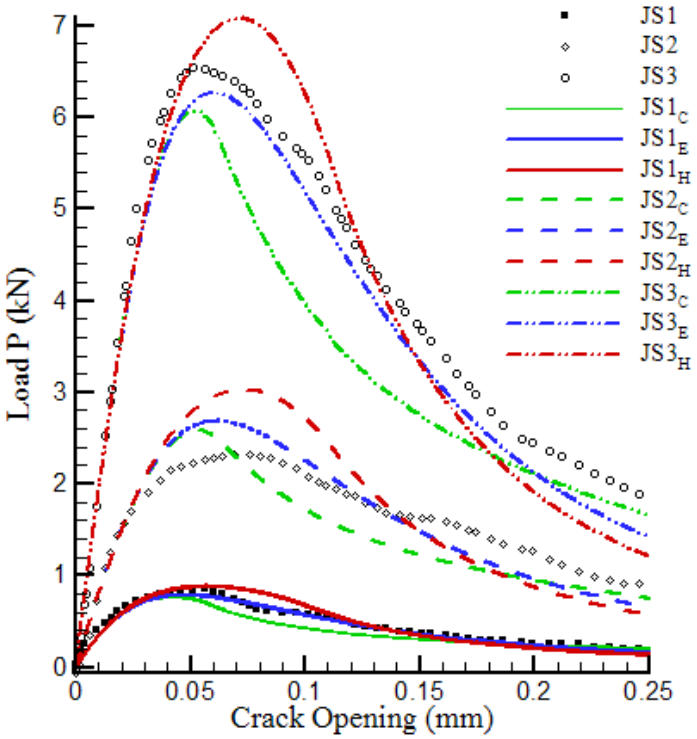

Figure 8: Load x crack opening compared with Jenq and Shah (1985b).

Second, the post-peak part of cohesive surface constitutive law does have an important effect not only in the post-peak behavior of the load x crack opening curve but also on the peak load itself. In all cases, Hilleborg et al. (1976) induce a somewhat more brittle behavior, with greater peak load and more abrupt drop overall (this behavior is emphasized in Figure 9).

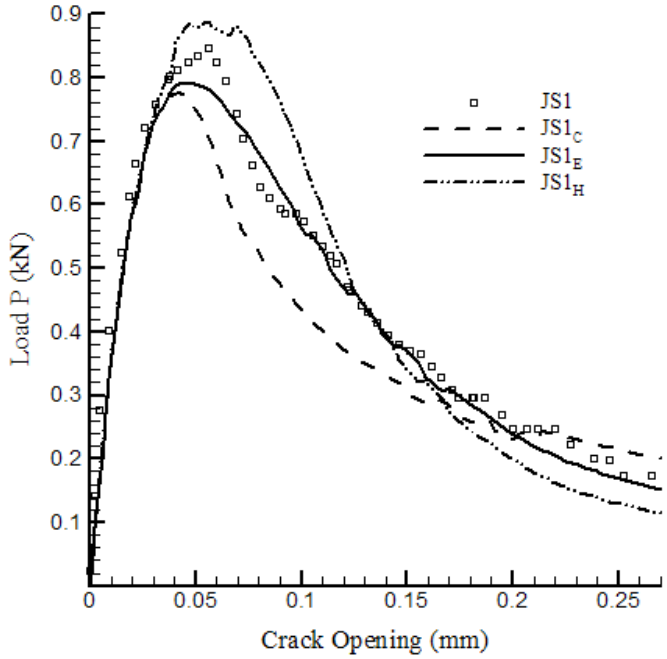

Figure 9: Various post-peak behaviors compared (case JS1, according Tables 3 and 4).

The more brittle behavior induced by Hilleborg et al. (1976) when compared to experiments, can be associated to the absence of energy fracture for large openings, when bridging and interlock play an important effect. The CEB-FIP Code Model (1990) and Xu (1999) present a greater toughness, especially at large openings. In general Xu's constitutive law fits better experimental results. A much better curve fitting with experiments can be obtained if w_s and σ_s (equations 6 and 7) are changed in the CEB-FIP Code Model.

5 CONCLUDING REMARKS

A cohesive model based on Hilleborg et al. (1976) principle of "fictitious crack model" was presented. The cohesive model must have also an elastic part, here called the pre-peak part of the cohesive constitutive law. It is here demonstrated, maybe for the first time, that:

- The elastic opening at peak traction (w_n) must be function of the characteristic length of FEs at the fracture zone.
- w_n can not be considered a constant, which can lead to a fake or numerical embrittlement of the concrete, in a limit case.

Regarding the post-peak part of the constitutive law:

- The curve proposed by Hilleborg et al. (1976) itself is not the best for concrete, mainly because it does not take into consideration the toughening effect of bridging/interlock for large crack openings.
- The post-peak curve with best fitting seems to be the one proposed by Xu (1999).

Evidences show that cohesive surface properties such as peak traction σ_{max} and fracture energy ϕ_n should be size dependent (see for instance Carpinteri et al. 2003). Even though this dependency was not explicitly considered here, still a good fitting was obtained with experiments. However the authors recognize the importance of the subject and a study in this regard is ongoing by them.

ACKNOLEDGMENTS

The author L.N.L. thanks CAPES, UFRGS and UNIOESTE for financial support.

REFERENCES

Barenblatt, G.I. The mathematical theory of equilibrium of crack in brittle fracture. *Advances in Applied Mechanics*, 7:55-129, 1962.

Bazant, Z.P. and Oh, B.H. Crack band theory for fracture of concrete. *Materials and Structures, RILEM*, 16:155-177, 1983.

Carpinteri, A. Decrease of apparent tensile and bending strength with specimen size: two different explanations based on fracture mechanics. *International Journal of Solids and Structures*, 25:407-429, 1989.

Carpinteri, A., Cornetti, P., Barpi, F. and Valente, S. Cohesive crack model description of ductile to brittle size-scale transition: dimensional analysis vs. renormalization group theory. *Engineering Fracture Mechanics*, 70:1809-1839, 2003.

Chandra, N., Li, H., Shet, C. and Ghonem, H. Some issues in the application of cohesive zone models for metal-ceramic interfaces. *International Journal of Solids and Structures*, 39:2827-2855, 2002.

Comité Euro-international du Béton. CEB-FIP Code Model 1990, *Bulletin d´Information num. 213/214*, Lausane, 1993.

De Borst, R., Remmers, J.J.C. and Needleman, A. Mesh-independent discrete numerical representations of cohesive-zone models. *Engineering Fracture Mechanics,* 73:160-177, 2006.

Dugdale, D.S. Yelding of stell sheets containing slits. *Journal of Mechanics and Physics of Solids*, 8:100-108, 1960.

Hilleborg, A. Modéer, M. and Peterson, P.E. Analysis of crack formation and crack growth in concrete by means of fracture mechanics and finite elements. *Cement and Concrete Research*, 6:773-782, 1976.

Jenq, Y.S. and Shah, S.P. Two parameter fracture model for concrete. *Journal of Engineering Mechanics*, 111:1227-1241, 1985a.

Jenq, Y.S. and Shah, S.P. A fracture toughness criterion for concrete. *Engineering Fracture Mechanics*, 21:1055-1069, 1985b.

Lens, L.N., Bittencourt, E. and d'Ávila, V.M.R. Quasi-fragile and fragile fracture behavior with the cohesive surface methodology. MECOM, Santa Fé, Argentina, 2006.

Needleman, A. Continuum Model for Void Nucleation by inclusion debonding. *Journal of Applied Mechanics* 54:525-531, 1987.

Riera, J. D. and Iturrioz, I. On the fracture analysis of concrete structures taking into consideration size effects. *18th Internation Conference on Structural Mechanics in Reactor Tecnology (SMIRT 18),* Beijing, China August 7-12, 2005.

Rose, J.H., Ferrante, J. and Smith, J.R. Universal binding energy curves for metals and bimetallic interfaces. *Physics Review Letters*, 47:675-678, 1981.

Rots. J.G. *Computational modeling of concrete fracture*. PhD Thesis, Delft University, 1988.

Shah, S.P., Swartz, S.E. and Ouyang, C. Fracture mechanics of concrete: applications of fracture mechanics to concrete, rock and other quasi-brittle material. Wiley-Interscience publication, 1995.

Tijssens, M.G.A., Sluys, B.L.J. and van der Giessen, E. Numerical simulation of quasi-brittle fracture using damaging cohesive surface. *European Journal of Mechanics A/Solids* 19:761-779, 2000.

Xu, X.P. and Needleman, A. Numerical simulations of fast crack growth in brittle solids. *Journal Mech. Phys. Solids*, 42:1397-1424, 1994.

Xu, X.P. Determination of parameters in the bilinear, Reinhardt´s non-linear and exponentially non-linear softeming curves and their physical meanings. Werkstoffe und Werkstoffprüfung im Bauwesen, *Hamburg, Libri BOD,* pp. 410-424, 1999.